**Title**
MEASUREMENT OP THE u~ POLARIZATION IN THE PROCESS n"" + p -9""S~+ K+



**Author**
Weldon, David Michael.

**Publication Date**
1967-02-01

UCRL-17152

# University of California

# Ernest O. Lawrence Radiation Laboratory

MEASUREMENT OF THE $\Sigma^-$ POLARIZATION IN THE PROCESS $\pi^- + p \rightarrow \Sigma^- + K^+$



Berkeley, California

## DISCLAIMER

UCRL-17152

UNIVERSITY OF CALIFORNIA

Lawrence Radiation Laboratory
Berkeley, California

AEC Contract No. W-7405-eng-48

# MEASUREMENT OF THE $\Sigma^-$ POLARIZATION IN THE PROCESS $\pi^- + p \rightarrow \Sigma^- + K^+$

David Michael Weldon
(Ph.D. Thesis)

February 1967

MEASUREMENT OF THE POLARIZATION OF THE $\Sigma^-$

IN THE PROCESS $\pi^- + p \rightarrow \Sigma^- + K^+$

Contents


Abstract . . . . . v

I. Introduction . . . . . 1

II. Experimental Method

A. General Method . . . . . 5

B. Experimental Apparatus . . . . . 8

1. Beam . . . . . 8

2. Polarized Target . . . . . 10

3. K Meson Detector . . . . . 12

4. Photography. . . . . 20

III. Data Analysis

A. Scanning and Measuring . . . . . 23

B. Kinematical Reconstruction . . . . . 24

C. Results. . . . . 27

IV. Discussion of Results. . . . . 36

V. Improving the Experiment . . . . . 43

Acknowledgments. . . . . 45

References . . . . . 46

# MEASUREMENT OF THE POLARIZATION OF THE $\Sigma^-$ IN THE PROCESS $\pi^- + p \rightarrow \Sigma^- + K^+$ *

David Michael Weldon

Lawrence Radiation Laboratory
University of California
Berkeley, California

December 1966

## ABSTRACT

The average polarization of the $\Sigma^-$ produced in the reaction $\pi^- + p \rightarrow \Sigma^- + K^+$ has been measured between center-of-mass angles $134^\circ$ and $166^\circ$ for an incident $\pi^-$ momentum of 1145 MeV/c. A polarized proton target was used and the $\Sigma^-$ polarization was found by measuring the difference in the production-rate of $K^+$ mesons for protons polarized along the production-plane normal and against it. Spark chambers were used to record the $\pi^-$ and $K^+$ trajectories, and the $\pi^-$ momentum was obtained from a magnetic spectrometer while the $K^+$ momentum was obtained from a range telescope. Each event was kinematically reconstructed in a one constraint fit to help eliminate events produced from protons bound in heavy nuclei of the target. The $\Sigma^-$ polarization was found to be $-0.36 \pm 0.46$ .

---

* Work done under the auspices of the U.S. Atomic Energy Commission.

# I. INTRODUCTION

Measurements of the polarization of the $\Sigma^-$ in the reaction

$$\pi^- + p \rightarrow \Sigma^- + K^+ \qquad (1)$$

are of current interest as much for the value they have in interpreting other experiments as for the light they shed on the reaction itself. Perhaps the major impetus for studying polarization in reaction (1) is that it would be helpful in an experiment making a further check of the Cabibbo theory of weak interactions.[1] In the decay

$$\Sigma^- \rightarrow n + e^- + \bar{\nu} \qquad (2)$$

the electron distribution relative to the $\Sigma^-$ polarization direction is predicted by this theory, but for this particular correlation to serve as a test, the $\Sigma^-$ polarization must be nonzero and if the polarization is not large its magnitude must be known. There are other correlations which do not involve the $\Sigma^-$ polarization, for example those involving the neutron polarization, but experimental difficulties make them difficult to measure. Because of the small branching ratio for decay process (2) ($1.3 \times 10^{-3}$), an abundant source of polarized $\Sigma^-$ is needed which could be supplied by reaction (1) if the $\Sigma^-$ hyperons were highly polarized.

Another experiment in which an abundant source of highly polarized $\Sigma^-$ would be helpful is the measurement of the decay parameters in

$$\Sigma^- \rightarrow n + \pi^- \quad . \qquad (3)$$

To measure all of the decay parameters it is necessary to measure the polarization of the decay neutron from polarized $\Sigma^-$. If the $\Sigma^-$ produced in reaction (1) is polarized, it is possible to measure both

the $\Sigma^-$ polarization and all of the decay parameters in process (3) from studies of the $\Sigma^-$ up-down decay asymmetry and the polarization of the decay neutron, but any additional information known about the polarization from other experiments aids in extracting more accurate values of the decay parameters.

Finally, knowledge of the $\Sigma^-$ polarization in reaction (1) makes possible a further check of charge independence in this reaction and the reactions

$$\pi^- + p \rightarrow \Sigma^o + K^o \quad . \tag{4}$$

and

$$\pi^+ + p \rightarrow \Sigma^+ + K^+ \quad . \tag{5}$$

Charge independence can be used to derive a set of triangle inequalities which put limits on the hyperon polarization in any of the three reactions, given the hyperon polarization in one of the others and the differential cross sections for all three.[2] The inequalities can be evaluated at any particular angle or for averages over a range of angles. These predicted limits can then be checked against experimental values.

At present very little work has been done on $\Sigma^-$ polarization in reaction (1) because of the difficulty in measuring it. This difficulty stems from the fact that the $\Sigma^-$, unlike the $\Lambda$ or $\Sigma^+$, does not reveal its polarization through decay modes in which the decay nucleon is correlated with the original hyperon spin. Over 99% of all $\Sigma^-$ decay as $\Sigma^- \rightarrow n + \pi^-$ but the decay is almost isotropic even if the $\Sigma^-$ is completely polarized.[3,4]

Several methods do exist for measuring the $\Sigma^-$ polarization

although they are more difficult than the up-down asymmetry method. One method requires measurement of the polarization of the decay neutron in process (3) and relates this to the polarization of the hyperon and to the weak interaction decay parameters.[5] This is a difficult experiment to do because it is necessary to see the scattering of a significant number of the decay neutrons in order to find their polarization. Another method requires measurement of the decay asymmetry of $\Sigma^+$ hyperons produced in the reaction

$$\pi^+ + D \rightarrow \Sigma^+ + K^o + (p) \qquad (6)$$

and invokes charge symmetry to equate the polarization of the $\Sigma^+$ to $\Sigma^-$ polarization in $\pi^- + p \rightarrow \Sigma^- + K^+$. In addition to charge symmetry, this method depends on the validity of the impulse approximation for neglecting effects of the spectator proton. Nussbaum et al.[6] have measured the average polarization in reaction (6) at an incident pion momentum of 1192 MeV/c and found it to be $-0.52 \pm 0.41$ for the average over all angles. They have also verified the validity of the impulse approximation inasmuch as the decay asymmetry of the $\Sigma^+$ produced in the $\pi^+ + D \rightarrow \Sigma^+ + K^+ + (n)$ was found to be similar to the decay asymmetry of $\Sigma^+$ produced in $\pi^+ + p \rightarrow \Sigma^+ + K^+$. A third method assumes the validity of the principle of charge independence and uses the triangle inequalities mentioned to put limits on the $\Sigma^-$ polarization, but usually the limits are not very restrictive. Using this method Doyle et al.[7] find $\sigma P_\Sigma(\cos\theta) = B_o \sin\theta + B_1 \sin\theta \cos\theta$ with $B_o = 1 \pm 10$ μb/sr and $B_1 = -18 \pm 25$ μb/sr for reaction (1) at an incident pion momentum of 1170 MeV/c. A fourth method -- the method

used in this experiment -- produces the hyperons from initially polarized protons and measures the ratio of production cross sections for the case of target protons polarized along the normal to the production plane ($\hat{k}_\pi \times \hat{k}_\Sigma$), and for the case against the normal. Details of the experimental method are discussed in the next section.

## II. EXPERIMENTAL METHOD

### A. General Method

According to the well-known formalism[8] the transition matrix for reaction (1) can be written as

$$M = g(\theta) + h(\theta)\, \hat{\sigma} \cdot \hat{n} \ , \tag{7}$$

and the initial density matrix as

$$\rho_i = \sum_{\mu=1}^{2} p_\mu \chi_\mu \chi_\mu^+ \ , \tag{8}$$

where $\chi_\mu$ is a spinor representing the spin state of the proton, $p_\mu$ is the relative probability for the proton to be in state $\chi_\mu$, $\hat{n} = \hat{k}_\pi \times \hat{k}_\Sigma$ is the normal to the production plane, $\hat{\sigma}$ is a vector whose components are the Pauli spin matrices, and $h(\theta)$ and $g(\theta)$ are functions of the production angle and energy. Equation (7) takes the relative intrinsic parity of the $K\Sigma$ system to be the same as that of the $\pi p$ system in accordance with the results of several groups of experimenters.[9,10] The choice of the direction of the normal to the production plane is the one most frequently used in the literature. To be specific, the $\hat{z}$ axis is taken as the axis of quantization and $\hat{n}$ is along $\hat{z}$. The final density matrix is given by

$$\rho_f = M\, \rho_i\, M^+ \ , \tag{9}$$

the cross section by

$$I_f(\theta) = \frac{\mathrm{Tr}\rho_f}{\mathrm{Tr}\rho_i} \ , \tag{10}$$

and the polarization of the $\Sigma^-$ by

$$P_\Sigma(\theta) = \frac{\mathrm{Tr}\rho_f \sigma_z}{\mathrm{Tr}\rho_f} \ . \tag{11}$$

In the case of scattering from an unpolarized target the initial density matrix is

$$\rho_i = \begin{pmatrix} 1/2 & 0 \\ 0 & 1/2 \end{pmatrix} ,$$

which when used with equations (7) through (11) yields the reaction differential cross section

$$I_0(\theta) = |g|^2 + |h|^2 , \tag{12}$$

and the $\Sigma^-$ polarization,

$$P_\Sigma(\theta) = \frac{2\mathrm{Re}\, h^* g}{|g|^2+|h|^2} . \tag{13}$$

In the case of scattering from a polarized proton target with the protons fully polarized in the $+\hat{z}$ direction the initial density matrix is

$$\rho_i = \begin{pmatrix} 1 & 0 \\ 0 & 0 \end{pmatrix}$$

and the cross section found in a similar manner is

$$I^+(\theta) = I_0(\theta)(1 + P_\Sigma(\theta)) . \tag{14}$$

When the protons are fully polarized in the $-\hat{z}$ direction the initial density matrix is

$$\rho_i = \begin{pmatrix} 0 & 0 \\ 0 & 1 \end{pmatrix}$$

and the cross section is found to be

$$I^-(\theta) = I_0(\theta)(1 - P_\Sigma(\theta)). \tag{15}$$

Combining equations (14) and (15) gives

$$P_\Sigma(\theta) = \frac{I^+(\theta) - I^-(\theta)}{I^+(\theta) + I^-(\theta)} \tag{16}$$

or in the case the target is only partially polarized by a fraction $P_T$

$$P_{\Sigma}(\theta) = \frac{1}{P_T} \cdot \frac{I^{+}(\theta) - I^{-}(\theta)}{I^{+}(\theta) + I^{-}(\theta)} \qquad (17)$$

Here the degree of target polarization has been assumed to be the same for protons polarized along the normal and against it, an assumption which is responsible for the simple form of equation (17) and which is well satisfied in this experiment. From equation (17) it can be seen that the polarization parameter can be measured by measuring the asymmetry in the production of $\Sigma^{-}$ hyperons produced from a polarized target as the target is polarized first along the normal and then against it.

In the particular target used in this experiment only 3% by weight of the target constituted free hydrogen and therefore $\Sigma^{-}$ hyperons were produced from protons bound in heavy nuclei in the target as well as from free protons. A large percentage of these quasi-elastic events can be eliminated by reconstructing each event kinematically and discarding those events where a large momentum (Fermi momentum) of the initial proton is indicated. Kinematic variables measured in this experiment are the momenta of the incoming $\pi^{-}(\vec{k}_{\pi}-)$ and the outgoing $K^{+}(\vec{k}_{K}+)$; the $\Sigma^{-}$ is not measured because it usually decays before reaching the spark chamber which could detect it. However, it is very probable that most of the detected $K^{+}$ correspond to the production of a $\Sigma^{-}$, since for a two body final state, $\Lambda$, $\Sigma^{+}$ or $\Sigma^{o}$ production by a $\pi^{-}$ incident on a nucleon is forbidden by charge conservation; and if an extra particle is produced, not only is the cross section smaller, but it is unlikely that the momentum and production angle of the $K^{+}$ will allow any confusion with simple associated pro-

duction. The magnitude of the $K^+$ momentum was found from its range in a range telescope made chiefly of copper, water, and plastic scintillator, while the magnitude of the $\pi^-$ momentum was measured in a magnetic spectrometer. Spark chambers recorded the particle trajectories. From $\vec{k}_\pi$ and $\vec{k}_K$ the mass of the unseen $\Sigma^-$ was calculated from the formula

$$M_\Sigma = \sqrt{E_\Sigma^2 - P_\Sigma^2} = \sqrt{(E_\pi + m_p - E_K)^2 - (\vec{k}_K - \vec{k}_\pi)^2} \quad , \tag{18}$$

where $E_\pi$ and $E_K$ are total energies of the $\pi^-$ and $K^+$, respectively, and $m_p$ is the mass of the proton. If the event was from a free proton the missing mass of the unseen particle would be 1197.2 -- the mass of the $\Sigma^-$ --, but if it was from a bound proton, the Fermi momentum would usually make the missing mass some other value. Of course some of the quasi-elastic events exactly simulate events from free protons, and this background was measured by means of a dummy target similar to the crystal target but lacking free hydrogen. With the exception of hydrogen the dummy target was made of elements of approximately the same atomic number and mixed in the same proportion as the crystal target. Both targets were of the same weight, but the dummy target was 1/3 larger in volume.

## B. Experimental Apparatus

### 1. Beam

The beam transport system, shown in Figure 1, was designed to deliver either a $\pi^-$ beam or a separated $\pi^+$ beam. The beam was tuned for negatively charged particles during the course of this experiment, and the separator was not used since its purpose was to remove the

Fig. 1. Schematic diagram of the beam transport system. Polarity of the quadrupoles was arranged so that $Q_1$, $Q_3$, $Q_5$, $Q_6$, $Q_9$, and $Q_{11}$ caused the beam to converge horizontally while $Q_2$, $Q_4$, $Q_7$, and $Q_{10}$ caused it to diverge horizontally. $Q_8$ was not activated.

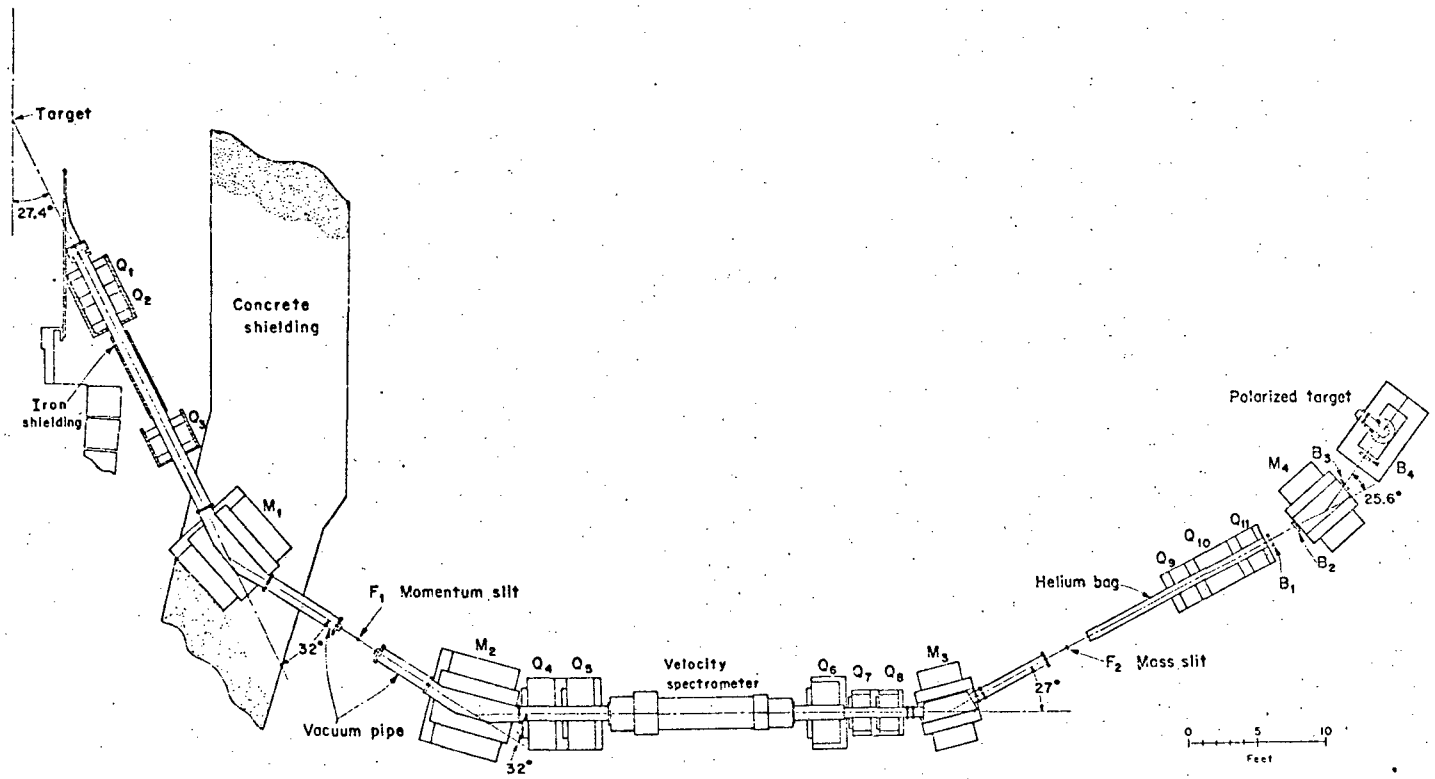


MUB-13684

large contamination of protons present when the beam was tuned for positively charged particles. The final image size was about 1.1 inch vertically by 1.3 inch horizontally (FWHM). Wire-orbits were used to find the value of the current set in each magnet expect for magnets $Q_1$, $Q_2$, $Q_3$, and $M_1$ where the currents were set empirically to obtain the maximum flux of $\pi^-$ mesons on the polarized target. For each event the momentum of the $\pi^-$ was obtained from its bending angle through $M_4$ as measured by spark chambers $B_1$ through $B_4$ positioned before and after $M_4$. In order to improve the precision of the momentum measurement, magnet $M_4$ was shimmed to make the integral of magnetic flux over particle trajectories ( $\int Bd\ell$) more uniform. The error in measuring the momentum due to variation of $\int Bd\ell$ was of the order $\pm$ 0.25%. Momentum spread of the beam was measured at $\pm$ 1.5%. Limits on the accuracy with which tracks in the beam spark chambers could be measured as well as spatial variation of the magnetic field of $M_4$ placed a limit estimated at $\pm$ 0.6% on the accuracy with which the relative momentum could be measured for each particle, but this was adequate for checking the momentum spread of the beam and later reconstructing each event kinematically. Typical beam rates were of the order of $10^5$ $\pi^-$ per Bevatron pulse with a spill of 300 msec. The momentum of the beam at the center of the polarized target was 1145 MeV/c..

2. Polarized Target

The polarized target used in this experiment was made of $Nd^{142}$ doped (0.2%) crystals of $La_2Mg_3(NO_3)_{12} \cdot 24\ H_2O$ in which the protons of

the water of hydration were polarized by the method of dynamic nuclear orientation.[11] This method first polarizes "electrons" of the $Nd^{142}$ ions by the application of a large magnetic field while the crystals are held at liquid helium temperatures; then the polarization is transferred from the electrons to the protons by saturating forbidden microwave transitions. Targets of this type have been discussed elsewhere[12-14] and only a few of the specifications of this target are quoted here. The four crystals used formed approximately a one-inch cube of weight 19.2 gms, and were cooled to a temperature of $1.2^{\circ}K$ in a magnetic field of 18.4 kilogauss. The microwave frequencies applied to polarize the protons at this magnetic field are in the neighborhood of 71 GHz, and the protons can be polarized either along the production plane or against it by 0.2% changes in the microwave frequency. By convention, the terms positive or negative enhancement are used to describe the condition of the target in which more protons are in the higher or lower of the two energy states, caused by the interactions of the proton's magnetic moment with the externally applied magnetic field. Because the magnetic field is along the production-plane normal, negative enhancement corresponds to positive proton polarization. i.e. protons polarized along $\hat{n}$. Nuclear magnetic resonance (NMR) techniques were used to measure the target polarization. Roughly speaking, the size of the NMR signal is a measure of the target polarization and absolute calibration is accomplished with so-called thermal equilibrium (TE) signals--NMR signals obtained from the target with the microwaves turned off and

for which the degree of polarization is calculable from the temperature of the crystals and the strength of the polarizing magnetic field. During the course of the experiment the sign of target polarization was changed approximately every two hours and the NMR detection system was calibrated every three days to avoid false asymmetries caused by long-term changes in the efficiency of any of the experimental apparatus. The average value of the target polarization over all data runs was found to be $0.37 \pm 0.04$ for positive enhancement and $0.38 \pm 0.04$ for negative enhancement. In other experiments under similar operating conditions the target polarization has often averaged as high as 0.48, however it has not been possible to demonstrate that measurements of the target polarization in this experiment are in error. The assigned error in target polarization is a systematic error due to variation of the tuning and sensitivity of the NMR equipment, and inaccuracy in measuring the crystal temperature while taking TE signals.

3. K Meson Detector

a. Method of Operation

The arrangement of the spark chambers and counters used to detect $K^+$ mesons is shown in Fig. 2 and details of their construction are given in Tables I and II. The beam of $\pi^-$ mesons passed through counter $S_1$ and D, and through a hole in anti-counter $A_1$ which vetoed events in which the pion missed the target. Counter D was connected to a circuit $(\bar{D}_c)$ which vetoed events in which two particles arrived in a period of 0.45 μsec in order to decrease the

Table I. Details of Counters

| Counter | Dimensions | Photomultipliers | Remarks |
|---|---|---|---|
| $S_1$ | 3 1/2" diam 1/4" thick | 7746 | |
| $S_3$ | 11" x 11" x 1/2" | two 7850's | |
| $A_1$ | 16" x 3 1/2" x 3/4" with 1 1/2" diam hole | 6810A | |
| $A_2$ | 10" x 2 1/2" x 1/2" | 7264 | |
| D | 5" diam 1/4" thick | 6810A | |
| $C_1$ | 12 1/8" x 12 1/8" x 2 3/8" | Six 6655A's | Wavelength shifter added |
| $C_2$ | 12 1/8" x 12 1/8" x 2 3/8" | Six 6655A's | Wavelength shifter added |
| T | 14 1/2" x 12 1/2" x 14 1/2" | Four 58AVP's | Lined with MgO |
| $\mu_T, \mu_B$ | 16 3/8" x 16 3/8" x 3/8" | 7850 | |
| $\mu_L, \mu_R$ | 18 3/4" x 16 3/8" x 3/8" | 7850 | |
| $S_2$ | 10" x 10" x 1/2" | C70101 | |

Table II Details of Spark Chamber Construction

| Chamber | Dimensions | Gaps | Plate Thickness | Remarks |
|---|---|---|---|---|
| $B_1, B_2, B_3, B_4$ | 8" x 8" x 2" | Eight 1/4" | 2 mil Al. | Two dummy gaps |
| $B_5$ | 2" x $1\frac{1}{2}$" x $\frac{1}{2}$" | Two 1/4" | 1 | |
| $K_1$ | Front face 9" x 3" | Twelve 1/4" | 1 | |
| | Back Face 9" x $1\frac{1}{2}$" | | | |
| | Thickness 3" | | | |
| $K_2$ | 7" x 7" x $1\frac{1}{2}$" | Six 1/4" | 2 | Two dummy gaps |
| $K_3$ | 10" x 10" x $\frac{1}{2}$" | Six 1/4" | 2 | |
| $K_4$ | 14" x 12" x 3" | Eight 3/8" | 2 | |
| $MU_T$ $MU_B$ | 14 1/4" x 14" x 3" | Eight 3/8" | 2 | |
| $MU_L$ $MU_R$ | 16 1/4" x 14" x 3" | Eight 3/8" | 2 | |
| | | | | All chambers filled with 90% Ne, 10% He |

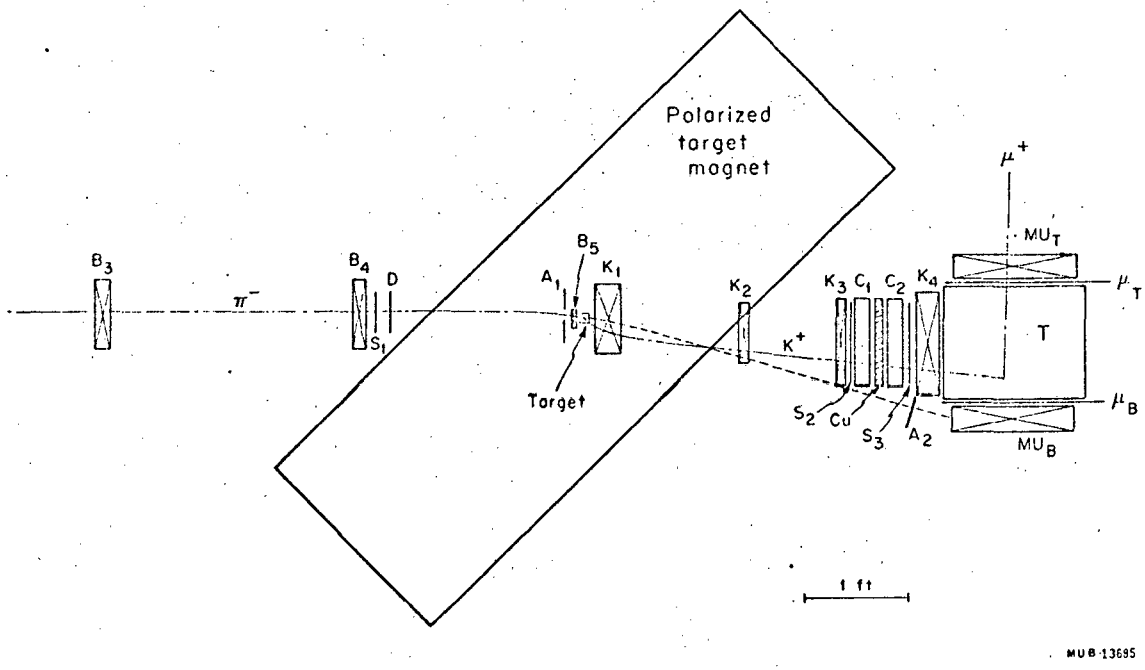


Fig. 2. Elevation diagram of the counter and spark chamber arrangement.

number of double tracks in the beam spark chambers. This device was operating for only about half of the experiment. On the average, $\bar{D}_c$ vetoed 9% of the total number of events which would have been recorded if this circuit were absent. $K^+$ mesons produced in the target passed through scintillators $S_2$ and $S_3$, through water-filled Čerenkov counters $C_1$ and $C_2$, and stopped in the large water-filled Čerenkov counter T. The Čerenkov threshold for water is $\beta = 0.75$ so the $K^+$ mesons $(0.7 \leq \beta \leq 0.75)$ did not trigger anti-counters $C_1$ and $C_2$, but elastically scattered $\pi^-(\beta \sim 0.99)$ and protons $(0.81 \leq \beta \leq 0.83)$ did. The 1.33 inch copper block degraded the momentum of the $K^+$ mesons so that they would stop in T. Once in T, a $K^+$ meson decaying by either $K_{\pi 2}$ or $K_{\mu 2}$ decay produced a charged particle with $\beta$ high enough to trigger T. If the particle passed through a side of T covered by one of the four $\mu$ counters it would also trigger a $\mu$ counter. The T signal and the sum of the $\mu$ counter signals $(\mu_{sum})$ were put into a coincidence circuit whose output was in turn put into the master trigger coincidence circuit which triggered the spark chambers. Output signals from the T-$\mu_{sum}$-coincidence were timed into the master trigger so that the $\mu$ and T counters would have to give signals delayed by 6 nsec from a "prompt" signal to generate a master trigger. This would further favor triggering on $K^+$ mesons because they decay with a 12 nsec lifetime. The width of the gate for the T-$\mu_{sum}$-coincidence was 50 nsec so that this signal had to fall within an interval between 6 and 56 nsec after a prompt signal from counters $S_1$, $S_2$, and $S_3$. Veto-counter

$A_2$ prevented triggering on events in which there was an unscattered beam particle and therefore helped eliminate accidentals. The master trigger can thus be written as

$$S_1 S_2 S_3 \bar{D}_c \bar{A}_1 \bar{C}_1 \bar{C}_2 \bar{A}_2 \, (T\mu_{sum})_{delayed} .$$

Once triggered, the spark chambers $B_1$ through $B_5$ recorded the $\pi^-$ trajectory, spark chambers $K_1$ through $K_4$ recorded the $K^+$ trajectory, while the $\mu$ chambers recorded the trajectory of the $K^+$ decay products. Signals of individual $\mu$ counters and of $\mu_{sum}$, as well as of counters $C_1$, $C_2$, $T$, $S_1$, $S_3$, and $A_2$ were photographed on a four-beam oscilloscope. The delay time on these pictures between any $\mu$ counter signal and the $S_3$ signal was later used as an additional check of the experiment since a plot of the number of events with any delay versus the delay time should show an exponential decay curve consistent with the $K^+$ lifetime.

b. Efficiency of Operation

Overall the K detector discriminated very effectively against $\pi^-$ mesons. Efficiency of the counters $C_1$ and $C_2$ alone for eliminating $\pi^-$ mesons was measured at 99.5% without the added discrimination of the delayed signal from counters $T$ and $\mu$. Discrimination against protons was poorer. The problem was that elastically scattered protons from the target had $\beta \sim 0.83$ which was close enough to the Čerenkov threshold for a significant number of them to slip by $C_1$ and $C_2$ without registering but giving a small signal in $T$. The required signal from the $\mu$ counters would also be present if the particle scattered

out of T or if it passed out through the back of T causing Čerenkov light in the μ counter light pipes. These light pipes covered 1/4 of the back of counter T . Either slewing of the T discriminator for small pulses or an accidental coincidence of two particles with the later one triggering the μ counters would delay the T-μ-coincidence by the required 6 nsec.

These general conclusions concerning the K detector efficiency can be supported by evidence obtained from analysis of the spark chamber pictures and from the distribution in the time delay between the $S_3$ and $\mu_{sum}$ signals photographed on the 4-beam scope. Inspection of the total of all scope pictures taken with the crystal target in place showed a μ counter time distribution which could be roughly fit by a prompt peak containing 58% of the events, a background uniformly distributed in time containing 28% of the events, and an exponential decay curve with a $K^+$ lifetime containing 14% of the events. The flat background is the sort of time distribution expected from accidentals, and when the spark chamber pictures were inspected, about 1/4 of them did have two or more tracks in the K chambers. Over half of the events in the prompt peak also had very small μ counter pulses and blank Mu spark chambers as they would if they were caused by particles which went out the back of counter T and triggered the counters by Čerenkov light in the light pipes. There is some uncertainty about the exact mechanism which caused the $\mu_{sum}$ signal to appear prompt on the scope pictures but the $\mu_{sum}$-T-

coincidence signal to be delayed into the master trigger by the required 6 nsec. Part of the answer could be slewing of the T discriminator for the small signals made by protons whose velocity was only a little over the Čerenkov threshold. Many of the T counter signals for these prompt events were much smaller than average.

Of all the pictures taken, only 1/4 were measurable since the remainder usually had 2 or more tracks in the K chambers or lacked Mu chamber tracks. The large number of pictures lacking Mu chamber tracks (1/2 of the total pictures taken) is explained by particles going out the back of counter T and triggering the μ counters by Čerenkov light in the light pipes, and by the fact that the μ counters were 35% larger than the Mu spark chambers. For the spark chamber pictures which were measured, particles which entered the K telescope could be identified by type from their bending in the magnetic field of the polarized target. This is so because of $K^+$ has half the momentum of an elastically scattered $\pi^-$ or proton, and protons can be distinguished from $\pi^-$ by the direction of curvature. This method showed that very few $\pi^-$ triggered the apparatus compared to the number of protons. For the measurable events 41% of the triggers were caused by $K^+$, 7% by $\pi^-$, and 25% by protons. It was not possible to identify 27% of the events and these events were probably caused by confusion of two different particles in different spark chambers or by the production of an extra particle in the final state which changed the momentum of the particle detected in the K telescope from that expected from either elastic

scattering or from reaction (1). The time distribution for the measured events could be adequately explained by a prompt peak containing 40% of the events, a flat background containing 22% of the events, and an exponential decay curve with about 12 nsec lifetime containing 38% of the events. Results of the kinematic reconstruction are in reasonable agreement with the timing information if the $K^+$'s are paired with events under the 12 nsec lifetime curve, the $\pi^-$ and protons as well as 1/4 of the unidentified particles are paired with prompts, and the rest of the unidentified particles are paired with the flat background in the timing distribution.

4. Photography

Two views in 90° stereo were collected from each spark chamber and brought to a 36 × 54 inch array of mirrors which was photographed at f/8.5 on Tri-X film. The distance of all the images was arranged to be 31.6 feet. The format of the spark chambers on each picture (Fig. 3) requires some comment. Because of space limitations between the pole tips of the polarized target, it was not feasible to place a single mirror on one side of either the $K_1$ or the $B_5$ chambers to obtain the side view. Side views were obtained by extending alternate gaps on alternate sides of the chambers and beveling each gap frame to a 45° angle so that light would be reflected through 90° into a direction perpendicular to the chamber plates. The shape of the $K_1$ chamber was tapered to prevent each gap from blocking the view of the one behind it. The $B_5$ had only 2 gaps so tapering was not necessary. This is the

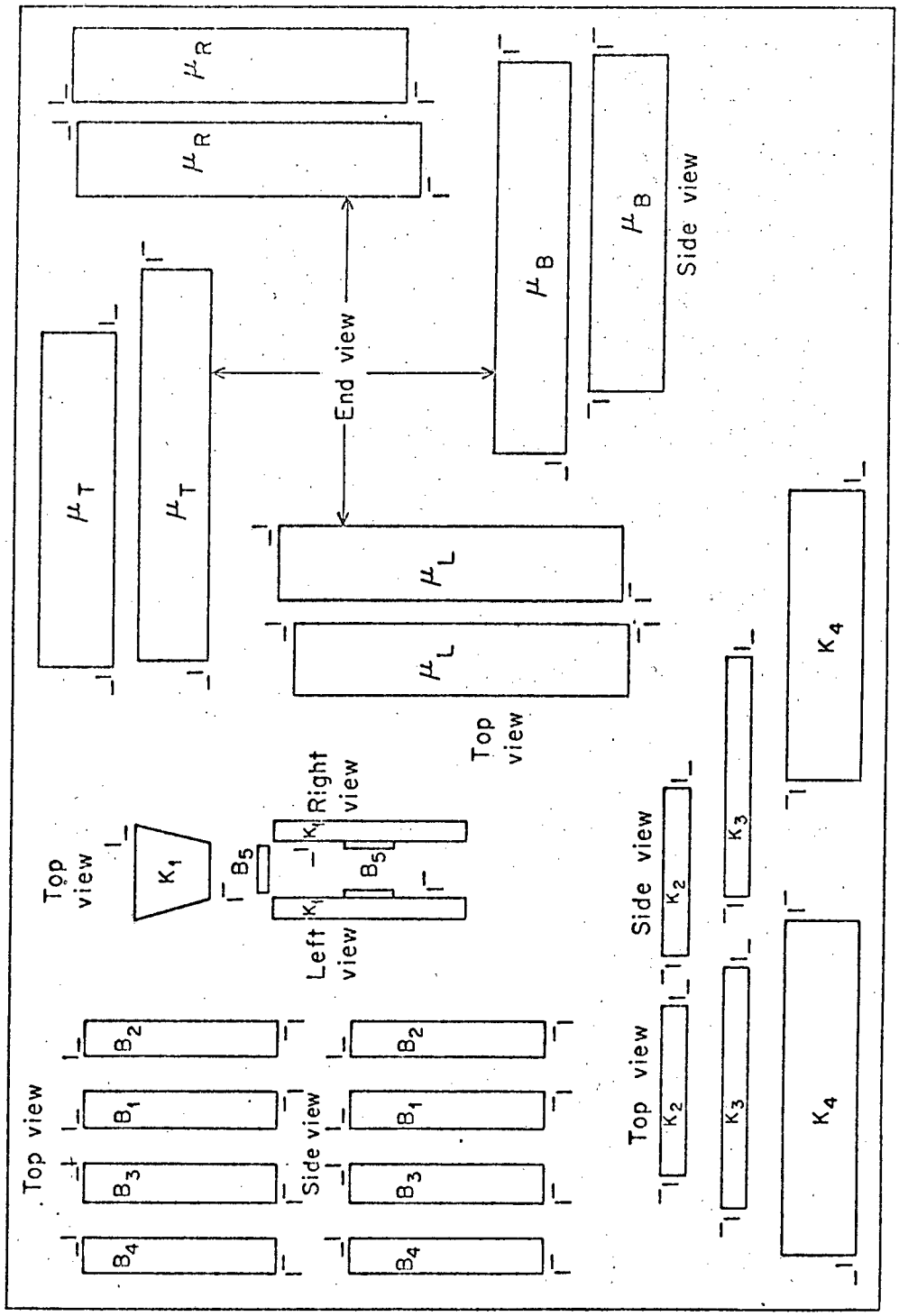


MUB 13686

Fig. 3. Spark chamber format as it appeared on each photograph. Roll and frame numbers appeared in the blank space in the lower right hand corner.

reason for the two side views of $B_5$ and $K_1$, one for even numbered gaps and one for odd, and for the shrinking of the width of these chambers by a factor of 4 in the side views. Fiducial lights whose position in real space was carefully surveyed are shown at two corners of each view, and binary lights in the blank space shown in the lower right hand corner of Fig. (3) gave the roll and frame numbers. The four beam scope was photographed with a DuMond oscilloscope camera on Tri-X film and roll and frame numbers were also recorded (in binary) on each frame.

# III. DATA ANALYSIS

## A. Scanning and Measuring

To avoid scanning bias, scanning criteria were made very loose and all film was scanned twice, each time by a different scanner. All events found by either scanner were measured and events which could not have been $K^+$'s were eliminated by the computer analysis. Each picture accepted for measuring was required to have the following qualities:

(a) Each spark chamber track had a mimimum of 2 gaps firing.

(b) Each view of the $K_2$, $K_3$, and $K_4$ chambers had only one new track but fainter tracks were permitted to be present.

(c) Multiple tracks were allowed in chambers $B_1$ through $B_5$, the Mu chambers, and in chamber $K_1$.

Events were allowed to have multiple tracks in the $K_1$ chamber because the magnetic field of the polarized target prevented removal of old tracks by the clearing field (200 V/inch). Ions drifted parallel to the chamber plates in the direction $\hat{E} \times \hat{B}$ rather than toward the plates so that at least one old track was often present. Even neglect- the effect of collsions, the ion drift velocity was calculated to be only 0.4 cm/μsec under the influence of the clearing field and the polarized target magnetic field. Frequently there were more tracks in the chamber than it could support, so that all tracks were discontinuous. The splitting of the side views of $K_1$ into two views, one for even and one for odd numbered gaps, added to the confusion and

measurement was sometimes impossible. Events were not rejected when the $K_1$ chamber was unmeasurable. Multiple tracks were allowed in the Mu chambers because the decay chain

$$K^+ \rightarrow \pi^+ + \pi^o \qquad \text{(branching ratio 0.21)}$$
$$\qquad\qquad\quad \downarrow \gamma + \gamma$$

would give two or three tracks as one or both of the gamma rays converted in T .

Since the entire beam passed through the chambers $B_1$ through $B_5$ , these chambers were also allowed to have more than one track. In chambers $B_1$ through $B_4$ , $Mu_1$ through $Mu_4$ , and chamber $K_1$ positions of up to three tracks were recorded in each, but only the single new track was recorded in $K_2$ , $K_3$ , and $K_4$ . Out of 6122 pictures taken as data with the crystal target or dummy target in place 1503 were measured. Examination of the final sample of $K^+$ events indicated that scanning criteria could have been profitably tightened. For these events the majority of gaps in each chamber had fired rather than the minimal two gaps and 85% of the time the beam chambers contained a single track per view.

## B. Kinematical Reconstruction

Each event was reconstructed by an IBM 7094 computer program which systematically checked each track against kinematics for the desired reaction. The calculation proceeded in the following manner: The point of intersection of tracks in a Mu chamber and $K_4$ chamber

was found and the momentum of the particle stopping in counter T was calculated from its range assuming it was a $K^+$. In the case of multiple tracks in the Mu chambers, the one most nearly intersecting the $K_4$ track was chosen. Using the momentum of the "$K^+$" meson and the track positions in the $K_2$ and $K_3$ chambers the particle trajectory was traced back through the magnetic field of the polarized target. If the particle was not a $K^+$ meson but a proton or $\pi^-$ meson elastically scattered out of the target and then scattered out of counter T, the real momentum would be about twice what it would be for a $K^+$. In the case of protons, the trajectory will still be convex viewed from below as it is for a $K^+$, but the trajectory will be flatter. Tracing a proton back to the target pretending it was a $K^+$ will make the trajectory fail to meet the incoming $\pi^-$ by about 1 inch. Elastically scattered $\pi^-$ have to be scattered upward in order to enter the K detector, and the magnetic field makes their trajectories concave viewed from below. Tracing back the trajectory using the same procedure as for the protons produces a trajectory almost 3 inches above the incoming $\pi^-$ at the target. These three kinds of events are easily separated and the background due to very inelastic processes is low. All events except those in the $K^+$ group were discarded. In the case of multiple tracks in chambers $B_1$ through $B_4$, over half the time the correct track could be chosen by seeing how close the projection of the track to the target came to the trajectory traced back from the K telescope.

The type of particle could then be identified in the manner discussed above. In those cases where the correct beam track could not be picked out the event was discarded. The production angle $\theta_K^*$ was also found from the $K^+$ and $\pi^-$ trajectories. Using the quantities $\vec{k}_\pi$ and $\vec{k}_K$ the mass of the unseen $\Sigma^-$ was calculated as described in Section II-A.

Several additional cut offs were applied to obtain a cleaner sample of events from unbound protons. In order to increase the resolution in missing mass the distance between the path of each "$\mu^+$ meson" leaving counter T and the path of the $K^+$ meson entering T was required to be less than 1.4 inch at the point of closest approach, and the angle between $K^+$ and $\mu^+$ tracks was restricted to the interval $30^\circ$ to $150^\circ$. To eliminate events not originating from the target crystals, each $\pi^-$ meson was obliged to pass through a 1.5 inch square centered on the target crystals. Although the $K_1$ chamber was not used, it was compared at this point with the predictions of the $K_2$ and $K_3$ chambers. In the usual case of multiple tracks in $K_1$, choice was made on the basis of how well they agreed with the angles predicted from the particle trajectory in chambers $K_2$ and $K_3$. For 85% of the events of the final $K^+$ sample, the scattering angle measured in the $K_1$ chamber agreed with the angle predicted from the $K_2$ and $K_3$ chamber to within $\pm 0.5^\circ$. Also in 85% of the events the predicted and measured trajectories in $K_1$ came within 0.35 inch of intersecting. The quality of tracks in the $K_1$ chamber was clearly better than average for the final sample of $K^+$ events.

## C. Results

Figure 4 shows the distributions in missing mass for the final sample of $K^+$ events. The unshaded histogram contains positive and negative target polarization data added together and the shaded histogram contains the dummy target data. In order to normalize the dummy target distribution to the polarized target distribution according to the number of incident $\pi^-$ mesons, the dummy target data have been multiplied by a factor 4.2. This is the ratio of the number of incident $\pi^-$ for polarized target data to the number of incident $\pi^-$ for dummy target data. As has been mentioned, the dummy target had the same mass of heavy elements as the polarized target but had a slightly lower density. The effect of this difference in density is neglected in normalizing the dummy target data and in calculating the $\Sigma^-$ polarization, but will be more fully discussed later. The smooth curve is a Monte Carlo calculation of the missing mass distribution for the crystal target normalized to the actual number of events, while the dashed lines show what part is due to quasi-elastic events. Included in the Monte Carlo calculation is the estimated resolution of the experiment in missing mass which is taken as a Gaussian with $\sigma = 6$ MeV . Resolution in missing mass is calculated from the effect of Coulomb scattering in counter T on $\vec{k}_K$ , and the effect of Coulomb scattering in the polarized target and of inaccuracy in measuring spark chamber tracks on $\vec{k}_\pi$ and $\vec{k}_K$ . Events in the mass interval $1184 \leq$ missing mass $\leq 1210$ MeV will be taken to be in the "elastic" peak, which means that 2 standard

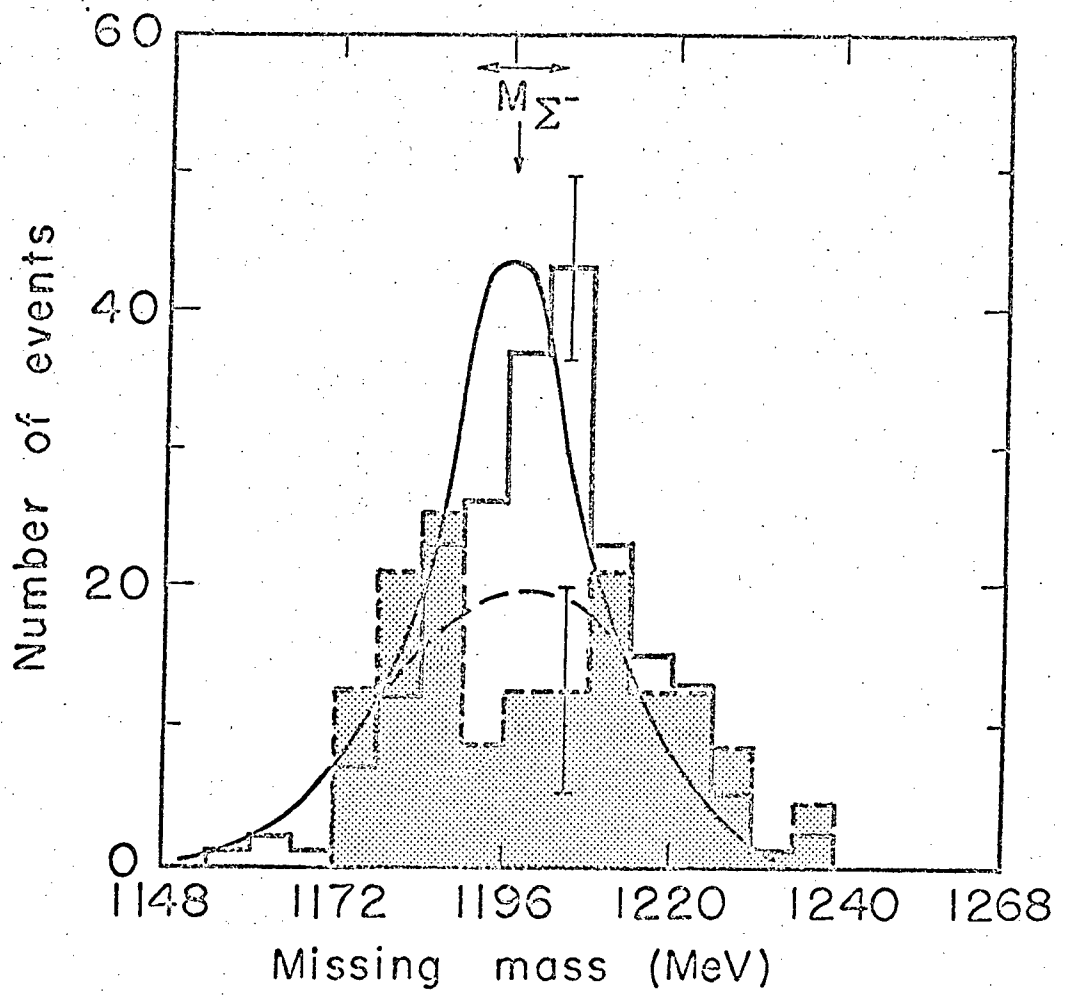


MUB-13982

Fig. 4. Missing mass for dummy target (shaded) and crystal target data normalized to the $\pi^-$ flux. The smooth continuous curve is a Monte Carlo calculation of the crystal target data, and the smooth dashed curve shows what part is due to events from protons bound in heavy elements of the target. Normalization of the Monte Carlo calculation is to the number of events in the crystal target data. The calculated resolution in missing mass is illustrated by an interval which should contain 68% of the events from free hydrogen in the crystal target.

deviations are taken on each side of the mass of the $\Sigma^-$, assuming a 6 MeV resolution. After subtracting the dummy target distribution (representing events from bound protons) from the crystal target data, there is a total of 72 events from free hydrogen. From considerations of production cross section, the useful solid angle subtented by counter T, and the probability that a $K^+$ will decay in counter T with decay products passing through one of the Mu spark chambers, a total of 81 events from free protons in the target is expected. Rejection of events because of too many tracks in the spark chambers and because of inefficiency of spark chambers and counters will further reduce this number, but the reduction is not expected to be very large. It should be remembered that the production cross section is only known to about 10%, and that because of the large background subtraction the statistical error on the 72 events is ±19. Agreement of the number of events expected with the number of events found can be considered to be satisfactory. The angular distribution in the center of mass of these 72 elastic events was found by subtracting the normalized dummy target distribution from the polarized target distribution. This distribution of elastic events is shown in Fig. 5 along with the shape of the differential cross section for reaction (1) normalized to the number of events. Cross section measurements at 1125[15] and 1170[16] MeV/c were interpolated to find the shape. As shown in this graph, $\theta^*_{\Sigma^-}$ is measured from the direction of the incoming $\pi^-$, and the data of this experiment measured the polarization between center-of-mass angles $134^\circ$ and $166^\circ$.

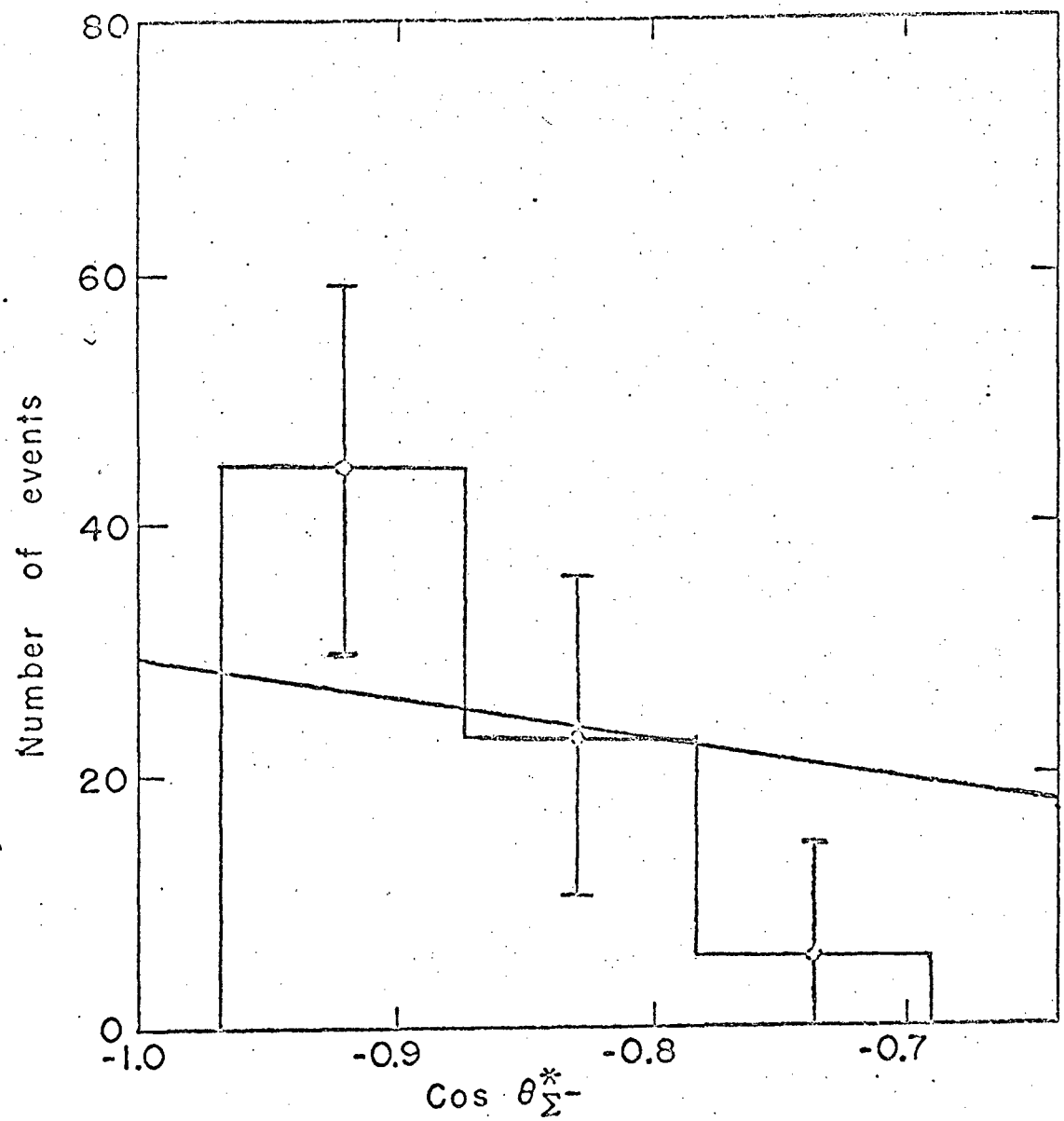


Fig. 5. Angular distribution of $K^+$ produced from unbound protons. The sample of $K^+$ events produced from unbound protons was obtained by subtracting properly normalized dummy target data from the polarized target data in the missing mass interval 1184 $\leq$ missing mass $\leq$ 1210 MeV. The differential cross section normalized to the number of events is plotted for comparison.

The decay time of all $K^+$ events from the polarized target and dummy target is plotted in Fig. 6 and is seen to compare very well with the $K^+$ meson lifetime of 12.3 nsec. Figure 7 shows the missing mass plotted separately for positive and negative target polarization along with the normalized dummy target data. The reason for the apparent shift of 6 MeV between positive and negative enhancement data is not understood. There appears to be no systematic difference between the two sets of data except the missing mass shift and the difference may well be a statistical fluctuation. Normalization of the dummy target data to both the positive and negative enhancement data was done with the same normalization factor (2.1) since the number of incident $\pi^-$ was about the same for both cases. The number of $\pi^-$ mesons incident on the target was $2.5 \times 10^9$ for positive enhancement $(M^+)$, $2.46 \times 10^9$ for negative enhancement $(M^-)$, and $1.2 \times 10^9$ for dummy target $(M^B)$.

Calculation of the $\Sigma^-$ polarization is now straightforward. The quantities

$$I^+ = \frac{N^+}{M^+} - \frac{N^B}{M^B} \quad , \tag{19}$$

and

$$I^- = \frac{N^-}{M^-} - \frac{N^B}{M^B} \tag{20}$$

are substituted in Eq. (17). Here $N^+$, $N^-$, and $N^B$ are the number of events in the selected missing mass internal for positive target polarization (i.e., negative enhancement), negative target polarization,

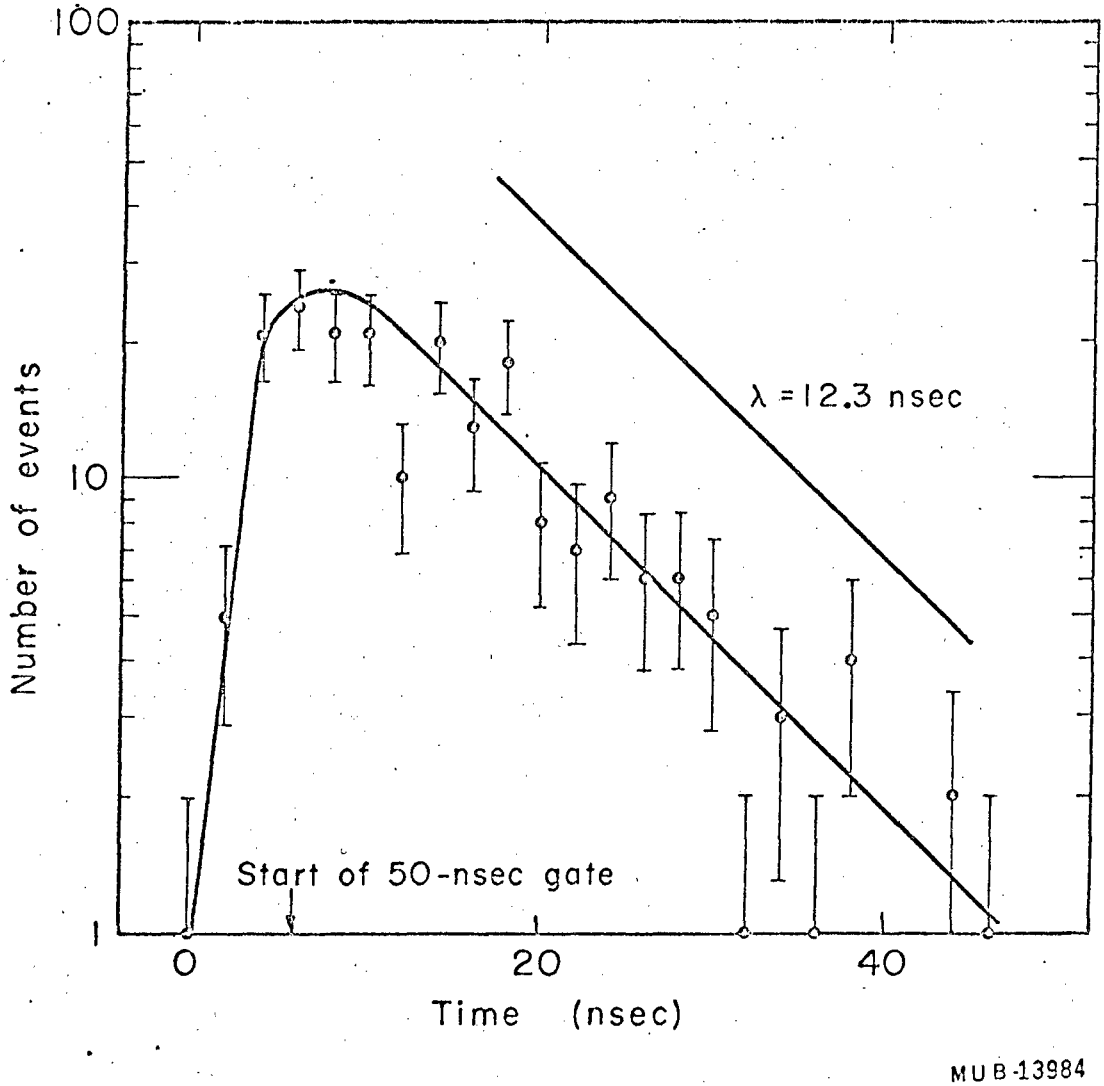


Fig. 6. Decay-time distribution of $K^+$ mesons for summed polarized target and dummy target data. A line with a slope corresponding to the $K^+$ lifetime of 12.3 nsec is shown for comparison.

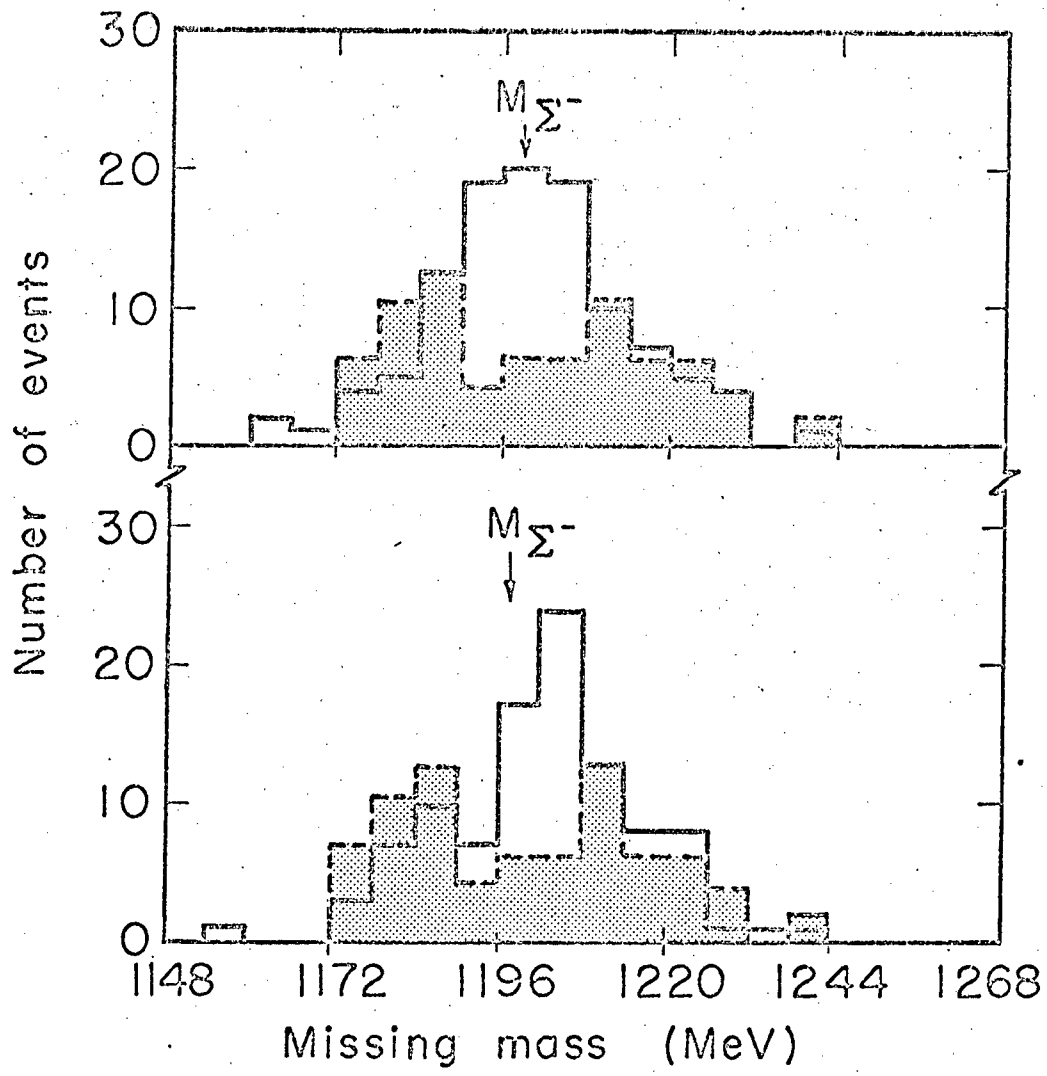


MUB-13983

Fig. 7. Missing mass plotted separately for positive and negative enhancement. Shaded histograms indicate dummy target data and all histograms are normalized to the $\pi^-$ flux. Top graph corresponds to positive enhancement, i.e., negative polarization of the $\Sigma^-$.

and dummy target. Each M is the corresponding flux of pions on the target. Using $N^+ = 75$ , $N^- = 64$ , $N^B = 16$ , and $P_T = 37.5$ as the average target polarization gives the $\Sigma^-$ polarization.

$$\bar{P}_{\Sigma^-} = - 0.36 \ . \qquad (21)$$

Statistical error in the polarization amounts to ±0.41, but in addition there are two principle sources of systematic errors. The 10% error in measuring target polarization has already been discussed. The other systematic error comes about from the manner in which the dummy target background is normalized to the crystal target data. Because the dummy target is only 0.75 as dense as the crystals, fewer events occur per unit area with a given incident flux of $\pi^-$ mesons. But, because the dummy target is larger it intercepts more of the beam, which tends to equalize production rates of events from bound protons in dummy and crystal targets. What is usually done to get the correct normalization is to take the shape of the dummy target data and normalize it to the quasi-elastic tails of the crystal data in whatever manner it is plotted. In this experiment the number of events in the inelastic tails of the dummy target is only 20 events which is too small to be useful. Another possibility would be to ignore the dummy target data and use the Monte Carlo calculation to estimate the quasi-elastic background. Agreement of the flux-normalized background with the Monte Carlo calculated background is certainly encouraging, but there are large uncertainties in the calculation too as a result of the over-simplified nuclear model used. The procedure finally adopted

was to calculate the polarization as if the flux-normalization was correct but increase the error to take account of the possibility of an incorrect normalization. The assumption that the number of events in the background normalized by $\pi^-$ flux should be increased by 1/3 (which is the maximum correction), yields $P_{\Sigma^-} = -0.50$ with an error of $\pm 0.59$. The final systematic error in normalization is reasonably taken as 0.2 which when combined with the other errors, all taken in quadrature, yields $\Delta P_{\Sigma^-} = \pm 0.46$ .

## IV. DISCUSSION OF RESULTS

The limited statistical accuracy of this experiment prevents us from making any strong statement concerning $\Sigma^-$ polarization. It may be worthwhile, however, to discuss in more detail those areas of investigation which could benefit by even a poor measurement of the $\Sigma^-$ polarization and to point out the significance of this experiment to these areas.

In the Introduction, it was mentioned that $\Sigma^-$ polarization had some significance in experiments measuring the decay parameters of the $\Sigma^-$. Cabibbo[17] has suggested a theory based on SU(3) which predicts that $\Sigma^-$ beta decay has the form $V + 0.65A$, where V and A stand for the vector and axial-vector hadron currents coupled to the lepton currents in the usual current-current interaction. A V-A theory gives a decay electron distribution from polarized $\Sigma^-$ which is almost isotropic, while a $V + 0.65A$ theory would give an electron distribution in which the electron usually goes in a direction opposite to the spin of the $\Sigma^-$.[18] Extensions of Cabbibo's theory by Pakvasa and Rosen[19] and by Brene et al.[20] also predict that the electron tends to go in a direction opposite the $\Sigma^-$ spin. Measurement of a large electron asymmetry would be a decisive proof against a V-A interaction, but the absence of any asymmetry would prove nothing unless the $\Sigma^-$ polarization were known to be large. The information that measurement of the electron asymmetry yields is the product of the polarization and a function of the parameters characterizing the decay. In order to

find the value of this function of the decay parameters, either the $\Sigma^-$ polarization must be known, or else the absolute value of the $\Sigma^-$ polarization and of this function of the decay parameters must both be near maximum, i.e. the electron asymmetry must be near maximum. This measurement of $\Sigma^-$ polarization would be more useful in investigating $\Sigma^-$ beta decay if it possessed greater statistical accuracy, but at least it does suggest that the polarization may be appreciable at 1145 MeV/c and is more likely negative than positive.

The relation of $\Sigma^-$ polarization to the decay parameters in $\Sigma^- \rightarrow \pi^- + n$ requires some discussion of these parameters. If the transition matrix is written in the form

$$M = A_s + A_p \hat{P}_{\Sigma^-} \cdot \hat{k}_p$$

the decay parameters can be defined as[21]

$$\alpha_- = \frac{2 \operatorname{Re} A_s^* A_p}{|A_s|^2 + |A_p|^2} \tag{22}$$

$$\beta_- \frac{2 \operatorname{Im} A_s^* A_p}{|A_s|^2 + |A_p|^2} \tag{23}$$

and

$$\gamma_- = \frac{|A_s|^2 - |A_p|^2}{|A_s|^2 + |A_p|^2} \quad . \tag{24}$$

There is some variation in the conventions used in defining $\alpha_-$ , $\beta_-$ , and $\gamma_-$ , and the definitions are not always consistent. For example, if $\hat{k}_\pi$ is used instead of $\hat{k}_p$ or $-A_p$ is substituted for $A_p$ in

the definition of $M$, a minus sign must be inserted in the definition of $\alpha_-$ if it is to have the same algebraic sign. The substitution of $-A_p$ for $A_p$ is usually not explicit but occurs when the final state is expressed as the sum of s- and p- waves but the density matrix formalism is not used. An advantage of the convention used here is that there is no minus sign relating the neutron helicity with the parameter $\alpha_-$ in Eq. (26), but much of the literature has the opposite sign.

The angular distribution of the decay neutron is given by

$$I = I_0(1 + \alpha_- \vec{P}_{\Sigma^-} \cdot \hat{k}_n) , \tag{25}$$

and the components of neutron polarization are given by

$$\langle \sigma_{k_n} \rangle = \frac{\alpha_- + \vec{P}_{\Sigma^-} \cdot \hat{k}_n}{1 + \alpha_- \vec{P}_{\Sigma^-} \cdot \hat{k}_n} (\hat{k}_n) \tag{26}$$

$$\langle \sigma_{\hat{k}_n \times \hat{P}_\Sigma} \rangle = \frac{\beta_-}{1 + \alpha_- \vec{P}_{\Sigma^-} \cdot \hat{k}_n} (\hat{k}_n \times \hat{P}_{\Sigma^-}) \tag{27}$$

and

$$\langle \sigma_{(\hat{k}_n \times \hat{P}_{\Sigma^-}) \times \hat{k}_n} \rangle = \frac{\gamma_-}{1 + \alpha_- P_{\Sigma^-} \cdot \hat{k}_n} \tag{28}$$

$$(\hat{k}_n \times \hat{P}_{\Sigma^-}) \times \hat{k}_n \ .$$

It should be remarked that the effects of final state interactions have been ignored in defining these components of neutron polarization. In this case these effects of final state interactions can be subtracted out from knowledge of the pion-nucleon phase shifts. The parameter

$\alpha_-$ has been found to be very small $(\alpha_- = -0.017 \pm 0.042)$,[22] a fact which is responsible for the lack of directional asymmetry in the decay $\Sigma^- \to n + \pi^-$. To measure $\alpha_-$, Eq. (25) was used with polarized $\Sigma^-$ obtained in the reaction $K^- + P \to \Sigma^- + \pi^+$ in the region of the $Y_o^*(1520)$. Polarization of the $\Sigma^-$ is not directly observable but can be obtained from phase shift studies of the reactions $K^- + P \to \Sigma^\pm + \pi^\mp$. Time reversal demands that $A_s$ and $A_p$ be relatively real (again ignoring final state interactions) so that from Eq. (22) and the vanishing of $\alpha_-$, either $A_s$ or $A_p$ is close to zero.

Several methods have been proposed to determine which one of them is close to zero. One method[23-25] measures the pion spectra in the radiative decays $\Sigma^\pm \to \gamma + n + \pi^\pm$ and invokes the $\Delta I = \frac{1}{2}$ rule of weak interactions to state that if one decay is by s-wave the other is by p-wave. Notice that this implies $\alpha_s \sim 0$ in one decay and $\alpha_p \sim 0$ in the other so there is no decay asymmetry in either decay. However, differences in the pion spectra of the two decays can be used to show which is s-wave. This experiment has been performed by Bazin et al., and concludes that s-wave is preferred for $\Sigma^- \to n + \pi^-$ by 2.7 standard deviations.[26] The other methods makes use of the fact that the polarization of the decay neutron in the decay processes $\Sigma^\pm \to n + \pi^\pm$ is different for s-wave and p-wave decays. For p-wave decay with the neutron momentum direction making an angle $\theta$ with the hyperon spin, the neutron polarization is in

the plane of $\hat{P}_n$ and $\vec{P}_\Sigma$ and at an angle $2\theta$ with the hyperon spin. For s-wave the neutron is polarized in the direction $\vec{P}_\Sigma$. This is easily seen by substituting the appropriate value of $\gamma$ in Eqs. (27) and (28). Simultaneously this method can measure the $\Sigma$ polarization but requires significant polarization for its success. The results of the present experiment can be combined with the results of Kofler,[27] who investigated the reaction $\pi^- + P \rightarrow \Sigma^- + K^+$ at 1125 MeV/c, but was not able to extract both the $\Sigma^-$ polarization and the $\gamma_-$ decay parameter because of poor statistics. However he was able to construct likelihood functions for s- or p-wave decay given any value of the hyperon polarization. Using the value of the polarization measured in this experiment and its associated error with these likelihood functions favors s-wave decay over p-wave decay by odds of 3 to 1. Berley et al.[28] have measured the polarization of the neutron in the decay $\Sigma^+ \rightarrow n + \pi^+$ and conclude that the decay is p-wave rather than s-wave by odds of $2 \times 10^4$ to 1. The $\Delta I = \frac{1}{2}$ rule again predicts that $\Sigma^- \rightarrow n + \pi^-$ is s-wave.

As has also been mentioned, $\Sigma^-$ polarization in reaction (1) can be used as a check of charge independence in the reactions (1), (4), and (5). That relationships should exist between the cross sections and polarizations in the three reactions is simply a result of having three reactions but only two I-spin amplitudes. Among other things charge independence shows[29] the inequality

$$2\cos^2 w_4 - 1 \bar{P}_1\bar{P}_5 \leq (1 - \bar{P}_1^2)^{1/2} (1 - \bar{P}_5^2)^{1/2} \qquad (29)$$

holds over a given angular region where $\bar{P}_1$ and $\bar{P}_5$ are average hyperon polarizations in reactions (1) and (5) and $w_4$ is the angle opposite the second side in the triangle $\Delta( \sqrt{\bar{\sigma}_1} , \sqrt{2\bar{\sigma}_4} , \sqrt{\bar{\sigma}_5} )$ . The symbols $\bar{\sigma}_1$ , $\bar{\sigma}_4$ , and $\bar{\sigma}_5$ stand for average cross sections for reactions (1), (4), and (5) over the given angular region. Charge independence also demands that the three quantities $\sqrt{\bar{\sigma}_1}$ , $\sqrt{2\bar{\sigma}_4}$ , and $\sqrt{\bar{\sigma}_5}$ satisfy a trigangle relation, i.e. that every sum of two of these quantities be greater than or equal to the third. If one of these quantities exactly equals the sum of the remaining two, the triangle is called flat; if one of these quantities is greater than the sum of the other two, the triangle fails to close and a violation of charge independence is indicated. It is easily proved that for a flat triangle $\bar{P}_1 = \bar{P}_5$ but when the triangle moves very slightly from flat, the relationship is satisfied for a wide range of $\bar{P}_1$ for any given $\bar{P}_5$ ; hence the inequalities are not of much value unless the triangle is flat. As a concrete example of the necessity of a flat triangle, consider a triangle with $w_4 = 180^\circ$ and $P_{\Sigma^-} = P_{\Sigma^+} = 0.5$ . If $w_4$ moves from $180^\circ$ to $170^\circ$ keeping $P_{\Sigma^+} = 0.5$ , the limits on $P_{\Sigma^-}$ are $0.20 \leq P_{\Sigma^-} \leq 0.76$ .

Data do not exist to check the charge independence triangle at 1145 MeV/c but the triangle has been constructed at 1125 MeV/c[30-31] and work is being done at 1170 MeV.c.[32-33] At 1125 MeV/c it appears

that the triangle fails to close by over 2 standard deviations in the range $-1 \leq \cos \theta_{\Sigma^-}^{*} \leq -0.8$ because the sides $\sqrt{\sigma_1}$ and $\sqrt{\sigma_5}$ are too short.[34] If charge independence is not violated in these angles, at least the triangle is very close to flat. Assuming the triangle is flat and charge independence holds, makes the $\Sigma^-$ polarization in reaction (1) equal to the $\Sigma^+$ polarization in reaction (4) which is known to be large and positive over $\pi^-$ momenta near 1145 MeV/c.[35] But the polarization found in this experiment is negative so there is still a hint of a violation of charge independence for reactions (1), (4), and (5) even if the triangle closes.

## V. IMPROVING THE EXPERIMENT

There are a number of ways in which the experiment could be improved if it were to be repeated. Since most of the error is statistical, one obvious recommendation is to collect more data. However, several minor modifications of the experimental apparatus could be made which would make data analysis easier and the collection rate faster. The number of pictures taken of events which were not caused by $K^+$'s , or which were not measurable should be reduced since they make scanning more difficult and reduce the data collection rate. There are several obvious ways of doing this. A veto-counter should be placed behind counter T to protect the μ counters' light pipes by vetoing events in which a particle went right through the entire apparatus. The μ counters should be better matched to the Mu spark chambers so that every particle going through a counter goes through a spark chamber. Whatever changes are necessary in the electronics should be made to prevent triggering on "prompt" events. One such change would be to widen the output pulse of the T discriminator to prevent it from setting the time of any coincidence.

The whole apparatus should be enlarged or else several modules of the same size arranged so that polarization could be measured over a greater angular range. Counter T should be lengthened so that in the missing mass distribution more of the tails caused by events from bound protons could be seen for normalizing the dummy target background subtraction. The resolution in missing mass could be increased by about a factor of 2 by increasing the distance between the spark chambers so

that $\vec{k}_\pi$ and $\vec{k}_K$ could be measured with more accuracy. It would also be helpful to reduce the number of multiple tracks in the chambers or else to make more complicated reconstruction programs to sort out the tracks. Some attempt was made to prevent double tracks in the spark chambers by vetoing events in which 2 particles arrived within 0.45 μsec, but this period is evidently not long enough. Spark chamber $K_1$ would work better if it were "poisoned", and the experimental arrangement should be such that the beam misses the K chambers as much as possible; in the present arrangement it went unnecessarily through the edge of chamber $K_2$ .

ACKNOWLEDGMENTS

I wish to express my deepest gratitude to Professor Herbert Steiner for his cousel and instruction throughout my graduate research, and my indebtedness to Professor Owen Chamberlain for his guidance during the preparation and performance of this experiment.

It is a pleasure to acknowledge the important contribution of Professor Gilbert Shapiro and Dr. Claude Schultz in their work in building the Berkeley polarized target and in many other aspects of this experiment.

My heartfelt thanks go to Dr. John Arens, Dr. Byron Dieterle, Dr. Paul Grannis, Dr. Leland Holloway, Dr. Michel Hansroul, and Dr. Claiborne Johnson for their labors in the design, data taking, and analysis of this experiment.

Also I wish to thank John Morton and Josephine Brosimer for their careful and patient work in scanning and measuring the photographic film and NMR charts.

The efforts of the Bevatron crew under the direction of Dr. Edward Lofgren as well as the efforts of all the technical support groups of the Lawrence Radiation Laboratory are also greatly appreciated.

This work was done under the auspices of the U. S. Atomic Energy Commission.

REFERENCES

1. N. Cabibbo, Phys. Rev. Letters 10, 531 (1963).

2. L. Michel, Nuovo Cimento 22, 203 (1961).

3. R. D. Tripp, M. Ferro-Luzzi, and M. Watson, Phys. Rev. Letters 9, 66 (1962).

4. Roger O. Bangerter, Angela Barbaro-Galtieri, J. Peter Berge, Joseph J. Murray, Frank T. Solmitz, M. Lynn Stevenson, and Robert D. Tripp, Phys. Rev. Letters 17, 495 (1966).

5. Richard R. Kofler, An Experimental Study of the Associated Production Reaction $\pi^- + P \rightarrow \Sigma^- + K^+$ (Ph.D. Thesis), University of Wisconsin, June 1964 (unpublished).

6. M. M. Nussbaum, R. W. Kraemer, A. Pevsner, M. Block, and A. Kovacs, Decay Asymmetries of Charged Sigma Hyperons, AEC, Division of Technical Information Extension Report NP12650, 1962 (unpublished); Mirko M. Nussbaum, Decay Asymmetries of Charged Sigma Hyperons (Ph.D. Thesis), Johns Hopkins University, 1961-1962 (unpublished).

7. Joseph C. Doyle, Ronald D. Levine, Jared A. Anderson, and Frank S. Crawford, Polarization of $\Sigma^-$ in the Reaction $\pi^- + P \rightarrow \Sigma^- + K^+$ and $\Sigma^-$ Decay Parameters, University of California Radiation Laboratory Report, UCRL-11916, Feb. 1965 (unpublished).

8. L. Wolfenstein and J. Ashkin, Phys. Rev. 85, 947 (1952).

9. Robert D. Tripp, Mason B. Watson, Massimiliano Ferro-Luzzi, Phys. Rev. Letters 8, 175 (1962).

10. Byron D. Dieterle, Experimental Determination of the KΣN Parity Using a Polarized Proton Target (Ph.D. Thesis), Lawrence Radiation Laboratory Report UCRL-17230, December 1966 (unpublished).

11. C. D. Jeffries, Dynamic Nuclear Orientation (Interscience Publishers, New York, 1963).

12. Claude H. Schultz, Scattering of 250 MeV Positive Pi Mesons from a Polarized Proton Target, (Ph.D. Thesis), UCRL-11149, Jan. 1964 (unpublished).

13. G. Shapiro, Prog. Nucl. Tech. Instr. 1, 173 (1964).

14. F. Betz, J. Arens, O. Chamberlain, H. Dost, P. Grannis, M. Hansroul, L. Holloway, C. Schultz, and G. Shapiro, Phys. Rev. 148, 1289 (1966).

15. See refernce 3, Page 60.

16. Jared A. Anderson, Strange Particle Production by 1170 MeV/c $\pi^-$ Mesons in Hydrogen (Ph.D. Thesis), University of California Radiation Laboratory Report UCRL-10838, May 1963.

17. Cf. reference 1, Table 1.

18. For closely related discussions concerning Λ decay see William T. Chu, Phys. Rev. 140, 685 (1965); V. G. Lind, T. O. Binford, M. L. Good, and D. Stern, Phys. Rev. 135, 1483 (1964).

19. S. Pakvasa and S. P. Rosen, Phys. Rev. 147, 1166 (1966).

20. N. Brene, L. Veje, M. Roos, and C. Cronstrom, Phys. Rev. 149, 1288 (1966).

21. For examples of some of the various conventions used in defining the decay parameters see e.g., R. D. Tripp, M. B. Watson, and

M. Ferro-Luzzi, Phys. Rev. Letters 9, 66 (1962); E. F. Beall, Bruce Cork, D. Keefe, P. G. Murphy, and W. A. Wenzel, Phys. Rev. Letters 8, 75 (1962); James W. Cronin and Oliver E. Overseth, Phys. Rev. 129, 1795 (1963); Frank S. Crawford, Jr., Strange Particle Decays, University of California Radiation Laboratory Report UCRL-10540, Nov. 1962 (unpublished).

22. See references 3 and 4.

23. Saul Barshay, Uriel Nauenberg, and Jonas Schultz, Phys. Rev. Letters 12, 76 (1964).

24. Robert D. Young, Masao Sugawara, and Teturo Sakuma, Phys. Rev. 145, 1181 (1966).

25. Ming Chiang Li, Phys. Rev. 141, 1328 (1966).

26. M. Bazin, H. Blumenfeld, U. Nauenberg, L. Seidlitz, R. J. Plano, S. Mavateck, and P. Schmidt, Phys. Rev. 140, 1385 (1965).

27. See reference 6, Page 68.

28. D. Berley, S. Herzbach, R. Kofler, S. Yamamoto, W. Heintzelman, M. Schiff, J. Thompson, and W. Willis, Phys. Rev. Letters 17, 1071 (1966).

29. Cf. reference 2, Eq. (17). Note that Eq. (18) is incorrect.

30. N. L. Carayannopoulos, G. W. Tautfest, and R. B. Willmann, Phys. Rev. 138, B433 (1965).

31. See reference 6, Page 66.

32. F. S. Crawford, F. Grard, and G. A. Smith, Phys. Rev. 128, 369 (1962).

33. Jared A. Anderson, Frank S. Crawford, Jr., and Joseph C. Doyle, Study of $\pi^- + P \rightarrow \Sigma^0 + K^0$ at 1170 MeV/c, University of California Radiation Laboratory Report, UCRL-16861, May 1966 (to be published).

34. See reference 6, Page 66.

35. See reference 29.